Inorganic Chemistry

pubs.acs.org/IC Article

Ligation of Boratabenzene and 9-Borataphenanthrene to Coinage Metals

Greta K. Wisofsky,[§] Katherine Rojales,[§] Xiaojun Su, Tyler A. Bartholome, Andrew Molino, Aishvaryadeep Kaur, David J. D. Wilson, Jason L. Dutton, and Caleb D. Martin*

Cite This: *Inorg. Chem.* 2021, 60, 18981−18989 Read Online

ACCESS | Metrics & More | Article Recommendations | Supporting Information

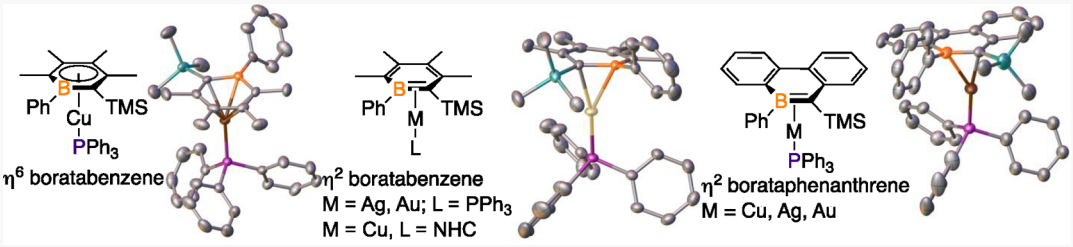

ABSTRACT: The reactions of boratabenzene and borataphenanthrene anions with group 11 Ph_3PMCl reagents furnished η^2 coordination complexes, with the exception of the copper boratabenzene species that adopted an η^6 mode. The binding of arene ligands to copper in an η^6 manner is rare, and altering the ancillary ligand on copper to an N-heterocyclic carbene switched the binding of the boratabenzene to η^2, indicating that such ligands are capable of vacating coordination sites. The η^2 coordination complexes bind side-on, akin to olefins, via a borataalkene unit, although with the carbon atom much more proximal to the metal center than boron.

INTRODUCTION

The bonding of unsaturated organic species to transition metals has been known since the pioneering synthesis of $[PtCl_3(C_2H_4)]^-$ in 1831 [**A** (Figure 1)].[1,2] The advent of metallocene chemistry is marked by the synthesis of ferrocene (**B**) in 1951,[3−7] and since these foundational discoveries, the bonding of unsaturated hydrocarbons with transition metals has been extensively studied.[8−13] Substituting a carbon atom for boron in benzene results in a six-membered anionic species, boratabenzene (**C**), that contains six π-electrons and can be considered a boron-containing hybrid of benzene and cyclopentadienide.[14] Cobalt boratabenzene complex **D** was disclosed by Herberich in 1970,[15] and these anionic BC_5 heteroarenes have been investigated as ligands for transition metals with complexes having diverse applications, including single-ion magnets as well as olefin polymerization and hydrogenation catalysts.[16−24]

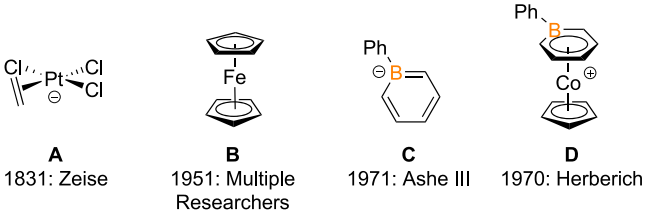

Figure 1. Hallmark organometallic compounds featuring organic π-ligands, boratabenzene, and the first boratabenzene metal complex.

Transition metal-bound monocyclic boratabenzene complexes adopt η^6-BC_5 coordination[25−34] except in rare examples in which π-donating substituents are bound to boron, resulting in η^3 or η^5 complexes.[21,35−38] Despite the vast array of known metal boratabenzene complexes, the coordination of monocyclic boratabenzenes to group 11 metals has remained unexplored. A polycyclic variant of boratabenzene, 9-borataphenanthrene (**1**), was recently demonstrated to coordinate to $Au(PPh_3)$ in an η^2 manner, the first example of an η^2 binding mode for a boratabenzene-containing species [**1**·$AuPPh_3$ (Figure 2)].[39] The central ring of the borataphenanthrene anion is considerably less aromatic than boratabenzene and has even been labeled as nonaromatic with a distinct borataalkene moiety in an ensuing computational study.[40]

In comparison to that in olefins, the π-bond in borataalkenes is highly polarized,[41,42] and accordingly, the Au−C bond distance in **1**·$AuPPh_3$ is much shorter than the Au−B bond,

Received: September 10, 2021
Published: December 8, 2021

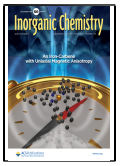

https://doi.org/10.1021/acs.inorgchem.1c02800
Inorg. Chem. 2021, 60, 18981−18989

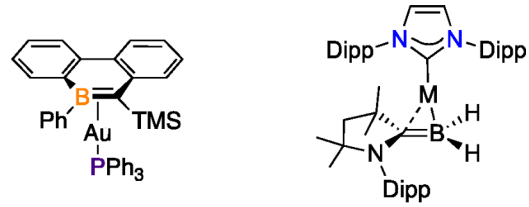

1·AuPPh$_3$ **E·CuIPr, M = Cu**
E·AgIPr, M = Ag
E·AuIPr, M = Au

Figure 2. η^2-Boratraphenanthrene gold complex **1**·AuPPh$_3$ and group 11 borataalkene complexes reported by Crimmin and co-workers (TMS, trimethylsilyl; Dipp, 2,6-diisopropylphenyl).

and the P−Au−C bond angle approaches linearity.[39] This species can be viewed as a relative to the α-boryl carbanions of copper and silver that have been labeled as key intermediates in coupling reactions.[42−61] In relation to **1**·AuPPh$_3$, Crimmin and co-workers reported copper, silver, and gold complexes (**E**·MIPr)[62−64] with a borataalkene not contained in an arene (**E**), and in this series, the borataalkene carbon was more distal from the metal in all three examples, which is the inverse of the boratraphenanthrene gold system **1**·AuPPh$_3$. In fact, the Crimmin species was labeled as η^1-boron bound to the metal for the gold, silver, and copper complexes, which contrasts the structural assignment to copper and silver α-boryl carbanions. Given the relevance of the copper and silver species to organic synthesis and the differences in gold complexes **1**·AuPPh$_3$ and **E**·AuIPr, we were inspired to pursue the other boratraphenanthrene species and to examine the chemistry of the monocyclic system, boratabenzene, with coinage metals.

RESULTS AND DISCUSSION

While several synthetic routes to boratabenzene exist,[16,18,65−74] we envisioned a ring expansion from an antiaromatic borole with a carbene source featuring a proton on the carbon atom and a subsequent deprotonation strategy could be a facile route for accessing boratabenzene species. The carbene insertion of diazomethane reagents into unsaturated BC$_4$ rings has been effective in preparing six-membered systems with a proton on an sp^3 carbon adjacent to boron.[75,76] The five aryl groups in the ring expansion product from pentaphenylborole would likely be problematic in metal complexation due to steric bulk and the potential of the phenyl substituents to interact with the metal. Accordingly, we selected a borole bearing methyl groups on the carbon atoms in the ring, 1-phenyl-2,3,4,5-tetramethylborole, which exists as a dimer at room temperature but upon heating sufficiently "cracks" and can undergo insertion chemistry.[77−80] The carbene insertion with trimethylsilyldiazomethane was complete after 16 h at 100 °C as confirmed by *in situ* ^{11}B NMR spectroscopy via the emergence of a singlet at 57.5 ppm in the spectrum and the disappearance of the peaks for the dimer at 67.5 and −6.6 ppm (Scheme 1). In the ^{1}H NMR spectrum, a singlet at 3.77 ppm was assigned to the allylic C−H proton for the six-membered boracycle **Int1**. Deprotonation with KHMDS furnished the corresponding boratabenzene with a diagnostic ^{11}B resonance at 37.4 ppm, and the ^{1}H NMR spectrum lacked the aliphatic C−H proton at 3.77 ppm. The identity was confirmed as the potassium boratabenzene species **2**·K by a single-crystal X-ray diffraction study that featured a 1,4-dioxane solvate coordinating to potassium (Figure 3).

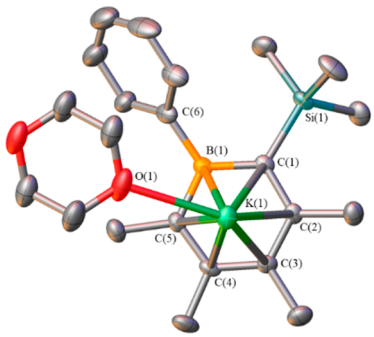

Figure 3. Solid-state structure of **2**·K with 1,4-dioxane coordinated to potassium. Only the asymmetric unit is shown. Hydrogen atoms have been omitted for the sake of clarity, and thermal ellipsoids are drawn at the 50% probability level. Selected bond distances (angstroms) and angles (degrees) are listed in Table 1.

The reactions of **2**·K with [(Ph$_3$P)CuCl]$_4$, [(Ph$_3$P)AgCl]$_4$, and (Ph$_3$P)AuCl reagents resulted in ^{31}P{^{1}H} NMR signals at 18.2 ppm, 20.9 and 17.5 ppm (^{107}Ag and ^{109}Ag isotopomers), and 36.2 ppm, respectively, as well as broad ^{11}B NMR resonances at 31.0, 32.4, and 33.4 ppm, respectively (Scheme 2). Single-crystal X-ray diffraction studies revealed complexation of the B=C bond to silver(I) and gold(I) in an η^2 coordination mode (**2**·AgPPh$_3$ and **2**·AuPPh$_3$, Figure 4), representing the first examples of η^2 coordination for a monocyclic boratabenzene. In contrast, the copper species, **2**·CuPPh$_3$, features boratabenzene coordination in an η^6 mode. Copper η^6-arene complexes are rare, only realized in 2015 by Hayton and co-workers.[81] To determine if the coordination of η^2-boratabenzene to copper could be achieved, a stronger donating ancillary ligand on copper was examined; specifically, the 1,3-bis(2,6-diisopropylphenyl)imidazol-2-ylidene (IPr) ligand was selected.[82−86] The reaction of (IPr)CuCl with **2**·K was complete after 15 min on the basis of *in situ* ^{11}B NMR spectroscopic monitoring as a new resonance at 32.4 ppm was observed, similar to the phosphine complex (**2**·CuPPh$_3$) at 31.0 ppm. A single-crystal X-ray diffraction study revealed that the IPr ligand rendered η^2-boratabenzene binding to copper [**2**·CuIPr (Figure 4)].

Scheme 1. Synthesis of Boratabenzene 2·K

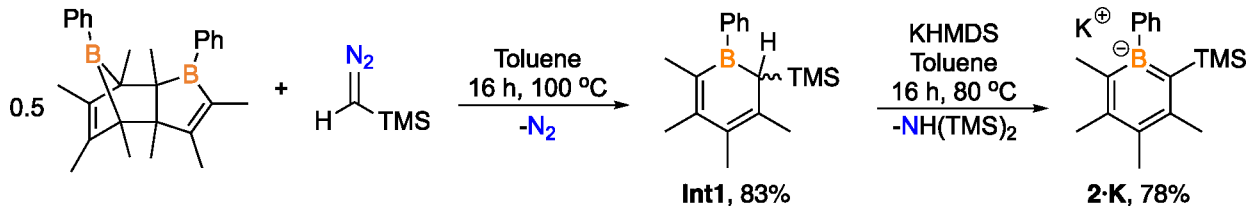

Int1, 83% **2·K**, 78%

https://doi.org/10.1021/acs.inorgchem.1c02800
Inorg. Chem. 2021, 60, 18981−18989

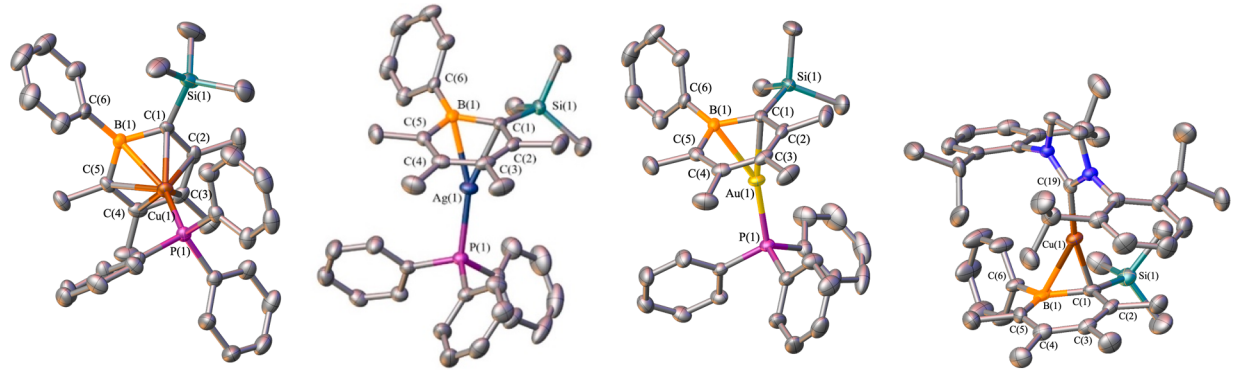

Figure 4. Solid-state structures of **2**·CuPPh$_3$, **2**·AgPPh$_3$, **2**·AuPPh$_3$, and **2**·CuIPr (from left to right, respectively). Hydrogen atoms and solvates have been omitted for the sake of clarity, and thermal ellipsoids are drawn at the 50% probability level. Selected bond distances (angstroms) and angles (degrees) are listed in Table 1.

Scheme 2. (a) Synthesis of 2·AgPPh$_3$,[a] 2·AuPPh$_3$,[b] and 2·CuPPh$_3$[c] and (b) Synthesis of 2·CuIPr

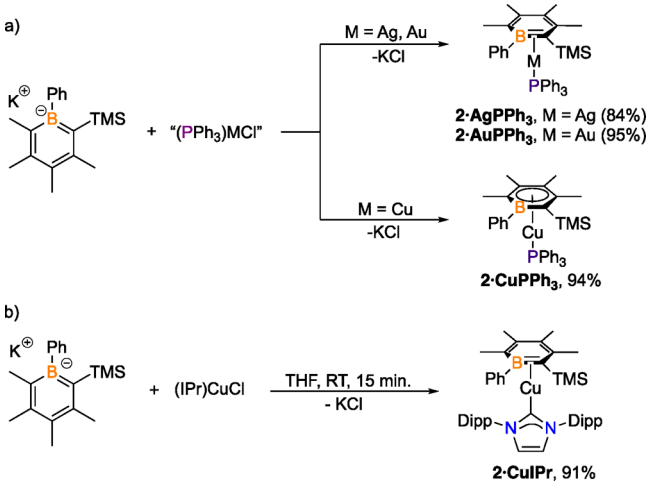

[a]Conditions for the synthesis of **2**·AgPPh$_3$: benzene/THF (4:1), rt, 10 min, then −35 °C to rt, 45 min. [b]Conditions for the synthesis of **2**·AuPPh$_3$: benzene/THF (4:1), rt, 3 h. [c]Conditions for the synthesis of **2**·CuPPh$_3$: benzene/THF (4:1), rt, 30 min.

We then turned our attention to the 9-boratraphenanthrene anion, **1**. The reactions of **1**·K with copper and silver [(Ph$_3$P)MCl]$_4$ reagents were monitored by *in situ* ^{31}P{^{1}H} NMR spectroscopy (Scheme 3). Signals were observed at 8.9 and 13.3 ppm in the NMR spectra for the reactions with [(Ph$_3$P)CuCl]$_4$ and [(Ph$_3$P)AgCl]$_4$, respectively, shifted downfield from those of the starting materials {−2.3 ppm for [(Ph$_3$P)CuCl]$_4$ and 9.4 ppm for [(Ph$_3$P)AgCl]$_4$}. The ^{11}B NMR signals for the products are broad singlets at 40.1 and 40.3 ppm, respectively, virtually unchanged from that of **1**·K (40.4 ppm). Single-crystal X-ray crystallographic studies revealed the identity as the η^2-borataalkene complexes **1**·CuPPh$_3$ and **1**·AgPPh$_3$ (Figure 5).

Scheme 3. Reactions of 1·K with [(Ph$_3$P)CuCl]$_4$ and [(Ph$_3$P)AgCl]$_4$[a]

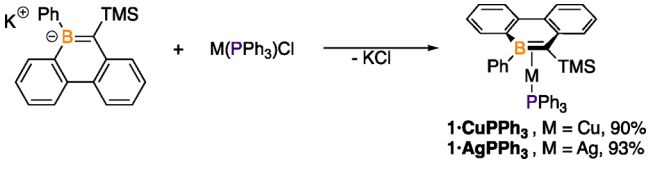

[a]Conditions for the synthesis of **1**·CuPPh$_3$: benzene/THF (3:1), rt, 10 min. Conditions for the synthesis of **1**·AgPPh$_3$: benzene/THF (4:1), -35 °C to rt, 30 min.

In all species, the endocyclic metrical parameters of the BC$_5$ rings are very similar for both potassium salts of the ligands and coinage complexes (Table 1). For the copper η^2-coordinated complexes, the copper is proximal to the trimethylsilyl-substituted carbon with Cu−C(1) bond distances similar for both complexes [2.020(3) Å for **1**·CuPPh$_3$ and 2.029(5) Å for **2**·CuIPr] while the bond is notably longer in the η^6-ligated boratabenzene complex [2.170(2) Å for **2**·CuPPh$_3$]. With regard to the Cu−B bond distances, the η^6-species has the shortest bond [2.248(2) Å for **2**·CuPPh$_3$; cf. 2.289(3) Å for **1**·CuPPh$_3$ and 2.351(5) Å for **2**·CuIPr]. The η^6-species, **2**·CuPPh$_3$, has a smaller discrepancy between the Cu−C(1) and Cu−B bond distances [2.170(2) and 2.248(2) Å, respectively] due to the aromatic binding. The η^2-coordinated species differ significantly from the **E**·CuIPr species (Figure 2), in which the boron interacted more strongly with the metal [Cu−B, 2.121(2) Å; Cu−C, 2.411(2) Å], and are related to the α-boryl carbanion complexes of copper.[64] The remaining Cu−C bond distances for the atoms in the boratabenzene ring all exceed 2.45 Å for **2**·CuIPr, whereas in η^6 complex **2**·CuPPh$_3$, they range from 2.292(2) to 2.344(2) Å.

Analogous to the copper η^2-species, the gold centers are much closer to the carbon center than the boron atom with the bond distances in the boratabenzene complex being closer in value [**1**·AuPPh$_3$: Au−B, 2.427(8) Å; Au−C(1), 2.188(7) Å; **2**·AuPPh$_3$: Au−B, 2.397(2) Å; Au−B, 2.247(2) Å].[39] In the silver species, the boratraphenanthrene species (**1**·AgPPh$_3$) follows the aforementioned trend of the metal−boron bond distances being greater than the metal−carbon bond distances, with the longest bond distances for the group 11 metals [Ag−B, 2.472(8) Å; Ag−C(1), 2.272(7) Å]. For the boratabenzene complex (**2**·AgPPh$_3$), the metal−ligand bond distances are very close [Ag−B, 2.3839(16) Å; Ag−C(1), 2.3586(14) Å]. The **E**·AgIPr and **E**·AuIPr complexes are significantly different with very short metal−boron bonds and long metal−carbon bonds [**E**·AgIPr: Ag−B, 2.287(3) Å; Ag−C, 2.633(3) Å; **E**·AuIPr: Au−B, 2.23(1) Å; Au−C(1), 2.68(1) Å].[64]

Theoretical studies were carried out to investigate the bonding and electronic structure. M06-2X/def2-TZVP[87,88] (CPCM solvation with THF solvent)[89] geometry optimiza-

https://doi.org/10.1021/acs.inorgchem.1c02800
Inorg. Chem. 2021, 60, 18981−18989

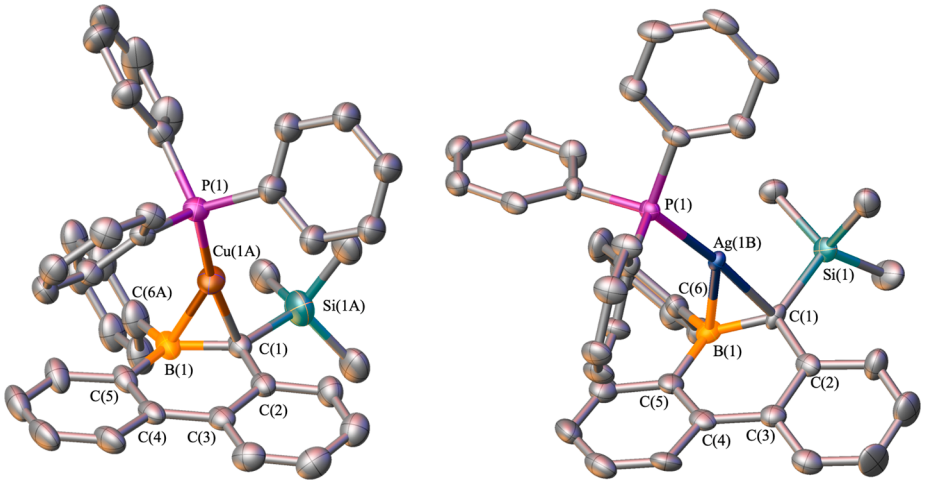

Figure 5. Solid-state structures of **1**·$CuPPh_3$ and **1**·$AgPPh_3$. Hydrogen atoms and the toluene solvate for **1**·$AgPPh_3$ have been omitted for the sake of clarity, and thermal ellipsoids are drawn at the 50% probability level. For disordered atoms, only the part with the highest occupancy is shown. Selected bond distances (angstroms) and angles (degrees) are listed in Table 1.

Table 1. Selected Bond Distances (angstroms) of the Borataphenanthrene and Boratabenzene Complexes from X-ray Diffraction Studies

	1·K[39]	**1**·$CuPPh_3$	**1**·$AgPPh_3$	**1**·$AuPPh_3$[39]	**2**·K	**2**·$CuPPh_3$	**2**·CuIPr	**2**·$AgPPh_3$	**2**·$AuPPh_3$
B(1)−C(1)	1.495(2)	1.508(4)	1.528(12)	1.504(11)	1.530(5)	1.541(3)	1.573(7)	1.541(2)	1.547(3)
C(1)−C(2)	1.450(2)	1.485(4)	1.471(11)	1.501(12)	1.432(4)	1.443(2)	1.470(6)	1.443(2)	1.465(3)
C(2)−C(3)	1.444(2)	1.438(4)	1.423(12)	1.435(11)	1.418(4)	1.412(4)	1.403(7)	1.399(2)	1.391(4)
C(3)−C(4)	1.471(2)	1.468(4)	1.466(14)	1.485(11)	1.423(5)	1.437(4)	1.430(7)	1.420(2)	1.428(4)
C(4)−C(5)	1.419(2)	1.409(4)	1.399(14)	1.424(12)	1.400(5)	1.408(4)	1.391(7)	1.405(2)	1.389(3)
C(5)−B(1)	1.553(3)	1.554(4)	1.584(13)	1.545(11)	1.523(5)	1.528(3)	1.517(8)	1.528(2)	1.532(3)
B(1)−M		2.289(3)	2.472(9)	2.427(8)		2.248(2)	2.351(5)	2.3839(16)	2.397(2)
C(1)−M		2.020(3)	2.272(7)	2.188(7)		2.170(2)	2.029(5)	2.3586(14)	2.247(2)
C(1)−Si(1)	1.8736(18)	1.868(5)	1.877(8)	1.891(12)	1.884(3)	1.896(3)	1.862(5)	1.8870(16)	1.893(2)

Table 2. M06-2X/def2-TZVP(CPCM, THF)-Calculated Bond Distances (angstroms) and Binding Energies (Δ*G*, kilojoules per mole) of the Borataphenanthrene and Boratabenzene Complexes

	1	**1**·$CuPPh_3$	**1**·$AgPPh_3$	**1**·$AuPPh_3$	**2**	**2**·$CuPPh_3$	**2**·CuIPr	**2**·$AgPPh_3$	**2**·$AuPPh_3$
B(1)−C(1)	1.482	1.507	1.512	1.527	1.513	1.534	1.532	1.536	1.541
C(1)−C(2)	1.450	1.473	1.482	1.493	1.415	1.434	1.445	1.432	1.460
C(2)−C(3)	1.433	1.437	1.433	1.430	1.415	1.434	1.410	1.432	1.460
C(3)−C(4)	1.466	1.476	1.476	1.481	1.402	1.421	1.429	1.413	1.394
C(4)−C(5)	1.417	1.428	1.421	1.418	1.416	1.432	1.399	1.426	1.440
C(5)−B(1)	1.558	1.574	1.572	1.571	1.395	1.413	1.528	1.411	1.389
BE[a]		63.6	120.6	135.8		89.9	118.6	133.2	121.3

[a]Binding energies are calculated for the **1**·$MPPh_3$ → $[MPPh_3]^+$ + $[\mathbf{1}]^-$ or **2**·$MPPh_3$ → $[MPPh_3]^+$ + $[\mathbf{2}]^-$ reaction (M = Cu, Ag, or Au).

tions[90] for the phosphine-ligated boratabenzene complexes are in good agreement with the solid-state structures for all three metal complexes. The optimized geometries of the silver and gold boratabenzene (**2**) complexes are consistent with η^2 bonding, while the geometry of **2**·$CuPPh_3$ indicates η^6 bonding. We were unable to locate a minimum for **2**·$CuPPh_3$ that was consistent with η^2 bonding, with efforts starting at a η^2 bonding geometry optimizing to η^6. This indicates that the η^6 geometry observed for **2**·$CuPPh_3$ is the thermodynamic minimum. In contrast, for the NHC-ligated copper species **2**·CuIPr, minima corresponding to both η^2 and η^6 could be optimized. Here the η^2 structure is the energetic minimum (consistent with the X-ray diffraction structure), with the η^6 complex being 5.0 kJ/mol higher in energy.

The impact of complexation of **1** and **2** by $MPPh_3^+$ or $CuIPr^+$ was investigated by computational means, with key bond distances and binding energies documented in Table 2. In general, complexation leads to a minor increase in the bond distances within the BC_5 ring, with the increase in bond distance generally larger in the **1**·$MPPh_3$ complexes than in the **2**·$MPPh_3$ complexes. For **1**, with a B(1)−C(1) distance of 1.482 Å, complexation with the group 11 metals increases the bond distance monotonically with the atomic number of the metal (**2**·$AuPPh_3$, 1.527 Å, Δ = 0.045 Å). Almost identical increases in bond distance are noted for the C(1)−C(2) bond, for which that of **2**·$AuPPh_3$ is the greatest (Δ*r* = 0.043 Å). Other bonds in the central borataphenanthrene ring do lengthen, but the changes are much less pronounced (at most 0.016 Å). In **2**, the B(1)−C(1) bond distance (1.513 Å)

https://doi.org/10.1021/acs.inorgchem.1c02800
Inorg. Chem. 2021, 60, 18981−18989

also increases upon complexation, with the greatest increase for **2**·AuPPh$_3$ (1.541 Å, Δ = 0.028 Å). The C(1)−C(2) bond increases slightly by 0.021 and 0.023 Å for Cu and Ag, respectively, but by nearly double that with Au (0.045 Å). Interestingly, in **2**·AuPPh$_3$ the C(2)−C(3) and C(4)−C(5) bond distances decrease upon complexation (Δ values of 0.006 and 0.008 Å, respectively) while they increase in **2**·CuPPh$_3$ and **2**·AgPPh$_3$ (Δ values of 0.011−0.019 Å). We hypothesize that complexation in **2**·AuPPh$_3$ enhances localized diene character. The variation in C−C bond distances in **2**·AuPPh$_3$ supports this hypothesis, with the diene bonds [C(2)−C(3) and C(4)−C(5)] being significantly shorter by 0.05−0.07 Å than the C(1)−C(2) and C(3)−C(4) bonds. In **2**·CuPPh$_3$ and **2**·AgPPh$_3$, the variation in C−C bond distances is much smaller (<0.02 Å), which suggests greater delocalization and less diene character.

Metal binding energies were determined from M06-2X/def2-TZVP(CPCM, THF)-calculated ΔG values for the **2**·MPPh$_3$ → [MPPh$_3$]$^+$ + [**2**]$^-$ and **1**·MPPh$_3$ → [MPPh$_3$]$^+$ + [**1**]$^-$ reactions (Table 2). In general, the metals bind more strongly to boratabenzene **2** than to borataphenanthrene **1**. For **1**·MPPh$_3$, there is a general trend of the binding energy increasing with the atomic number of group 11 metals (Cu, 63.6 kJ/mol; Ag, 120.6 kJ/mol; Au, 135.8 kJ/mol). The same trend is not observed for **2**·MPPh$_3$ (Cu, 89.9 kJ/mol; Ag, 133.2 kJ/mol; Au, 121.3 kJ/mol). Upon comparison of **1**·MPPh$_3$ and **2**·MPPh$_3$, for Cu and Ag the binding energy is greater in **2**·MPPh$_3$, while that trend is reversed for Au. The different coordination of **2**·CuPPh$_3$ (η^6) compared to that of **2**·AgPPh$_3$ and **2**·AuPPh$_3$ (both η^2) may be hypothesized to impact this trend. However, for **2**·CuIPr the energy difference between η^2 and η^6 complexes is only 5.0 kJ/mol, and hence, it is expected that the binding energy of **2**·CuPPh$_3$ will remain smaller than those of **2**·AgPPh$_3$ and **2**·AuPPh$_3$. It is suggested that **2**·AuPPh$_3$ is the exception, although high-level calculations together with explicit solvation would be required to provide definitive binding energies. As outlined above, bonding in **2**·AuPPh$_3$ increases the level of diene character in contrast to those of **2**·CuPPh$_3$ and **2**·AgPPh$_3$, which may rationalize the smaller than expected binding energy in **2**·AuPPh$_3$.

Energy decomposition analysis (EDA) was carried out at the B3LYP-D3(BJ)/TZ2P level of theory to probe the metal−complex interactions.[91,92] The results indicate that the interaction between the anionic heterocycle (boratabenzene or borataphenanthrene) and the metal cation is donor−acceptor in nature and predominantly electrostatic [ΔE_{elstat} = 60−65% (see the Supporting Information for numerical results)]. The electrostatic nature of these interactions enabled noncovalent interaction (NCI) analysis[93] of the bonding character (hapticity), which employed the M06-2X/def2-TZVP(THF, CPCM) geometries and electron density. For the borataphenanthrene complexes, the NCI surface is localized to the B−C(1) bond (analogous to the HOMO), consistent with η^2 bonding localized to the B═C bond. The NCI surface (Figure 6) for **2**·CuPPh$_3$ is equally distributed across all central ring atoms of boratabenzene, consistent with η^6 coordination. The **2**·AuPPh$_3$ and **2**·CuIPr complexes may be characterized as η^2 (localized to the B═C bond); for **2**·CuIPr, this description is consistent with the η^2 configuration being lower in energy than the η^6 configuration. The **2**·AgPPh$_3$ complex is intermediate between copper and gold and could be considered η^3 according to EDA.

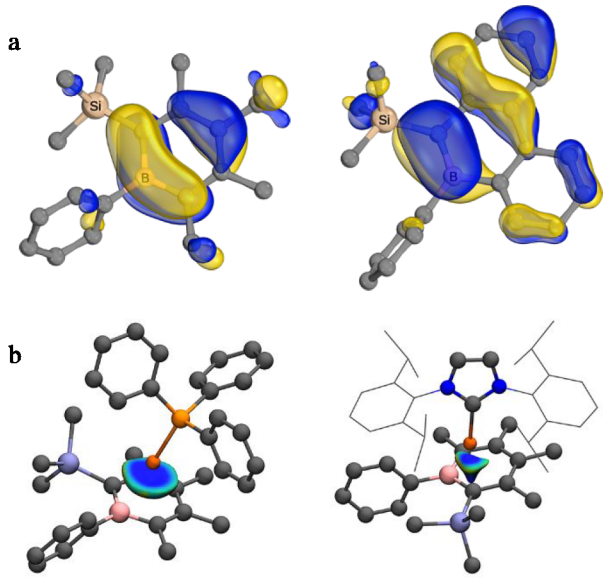

Figure 6. (a) HOMOs of [**2**]$^-$ (left) and [**1**]$^-$ (right). (b) NCI surfaces for **2**·CuPPh$_3$ (left) and **2**·CuIPr (right). Hydrogen atoms have been omitted for the sake of clarity. Iso value of 0.03.

The B3LYP-D3(BJ)/def2-TZVP(PCM solvation, SMD, THF solvent)-calculated NBO partial charges[94,95] of anions **1** and **2** indicate that the negative charge is more evenly distributed over the ring in **2**, which is consistent with the greater aromaticity of **2**. For **1**, there is a larger negative charge on the C-TMS carbon atom [−0.86 e vs −0.93 e (Table 3)]. This may help explain why boratabenzene allows for η^6 binding to copper in **2**·CuPPh$_3$, while for **1**, η^2 binding is observed for all complexes. Complexation of **1** by MPPh$_3$ consistently increases the magnitude of the charge on both the carbon and boron of the borataalkene moiety [C(1) and B(1)]. For **2**, complexation to copper and silver has little effect on the charge on C(1) and B(1) while binding to gold has a pronounced increase. The variation in atomic charges is consistent with the analysis of bond distances and the increased diene character for **2**·AuPPh$_3$. The frontier molecular orbitals (MOs) of uncomplexed anionic boracycles **1** and **2** indicate that the HOMO is π-symmetric, extended over the entire ring in the boratabenzene moiety but more localized to the endocyclic B═C bond in borataphenanthrene (Figure 6). The HOMO of **2** is higher in energy (−3.96 eV) than that of **1** (−4.18 eV), in line with the formation of more tightly bound complexes with **2**.[96] Finally, nucleus-independent chemical shift (NICS) scan[95] calculations at the B3LYP-D3(BJ)/def2-TZVP(PCM solvation, SMD, THF solvent) level of theory indicate that the boratabenzene ligand is more aromatic than the boron-containing ring of borataphenanthrene with NICS(1)$_{ZZ}$ values of −19.5 and −15.4 ppm, respectively. The increased aromaticity in boratabenzene is also consistent with it being able to accommodate η^6 coordination for Cu with PPh$_3$, while the less aromatic borataphenanthrene accommodates only η^2 coordination.

CONCLUSION

This study provides significant insight into the chemistry of boratabenzene and borataphenanthrene anions. An expedient synthesis of a monocyclic boratabenzene is disclosed via the insertion of carbene into a borole and a subsequent

https://doi.org/10.1021/acs.inorgchem.1c02800
Inorg. Chem. 2021, 60, 18981−18989

Table 3. Calculated NPA Charges of 1, 2, and Their Respective Metal Complexes

	1	1·$CuPPh_3$	1·$AgPPh_3$	1·$AuPPh_3$	2	2·$CuPPh_3$	2·$AgPPh_3$	2·$AuPPh_3$
B(1) charge	0.45	0.46	0.52	0.62	0.40	0.38	0.36	0.45
C(1) charge	−0.93	−0.96	−1.00	−1.03	−0.86	−0.87	−0.87	−0.95

deprotonation. The reactions of the group 11 PPh_3MCl reagents with the anions yielded η^2 coordination complexes for all borataphenanthrene species as well as for the gold and silver boratabenzene complexes with the general trend of shorter M−C bonds than M−B bonds. This is consistent with the polarization of the B═C bond, and the complexes can be related to complexed α-boryl anions proposed as catalytic intermediates in copper and silver coupling reactions. The triphenylphosphine copper boratabenzene complex binds in an η^6 manner but can be coaxed to η^2 upon modifying the ligand to a stronger N-heterocyclic carbene. These changes in hapticity suggest that η^6 boratabenzene species can free coordination sites by slippage, which could have implications for reactivity and catalysis.

■ ASSOCIATED CONTENT

Supporting Information

The Supporting Information is available free of charge at https://pubs.acs.org/doi/10.1021/acs.inorgchem.1c02800.

^1H, ^{13}C, and ^{11}B NMR spectra for all new compounds; FT-IR spectra; crystallographic data; computational details; and ligand competition studies (PDF)

Accession Codes

CCDC 2102905−2102911 contain the supplementary crystallographic data for this paper. These data can be obtained free of charge via www.ccdc.cam.ac.uk/data_request/cif, or by emailing data_request@ccdc.cam.ac.uk, or by contacting The Cambridge Crystallographic Data Centre, 12 Union Road, Cambridge CB2 1EZ, UK; fax: +44 1223 336033.

■ AUTHOR INFORMATION

Corresponding Author

Caleb D. Martin − *Department of Chemistry and Biochemistry, Baylor University, Waco, Texas 76798, United States*; orcid.org/0000-0001-9681-0160; Email: caleb_d_martin@baylor.edu

Authors

Greta K. Wisofsky − *Department of Chemistry and Biochemistry, Baylor University, Waco, Texas 76798, United States*

Katherine Rojales − *Department of Chemistry and Biochemistry, Baylor University, Waco, Texas 76798, United States*

Xiaojun Su − *Department of Chemistry and Biochemistry, Baylor University, Waco, Texas 76798, United States*

Tyler A. Bartholome − *Department of Chemistry and Biochemistry, Baylor University, Waco, Texas 76798, United States*

Andrew Molino − *Department of Chemistry and Physics, La Trobe Institute for Molecular Science, La Trobe University, Melbourne, Victoria, Australia 3086*; orcid.org/0000-0002-0954-9054

Aishvaryadeep Kaur − *Department of Chemistry and Physics, La Trobe Institute for Molecular Science, La Trobe University, Melbourne, Victoria, Australia 3086*

David J. D. Wilson − *Department of Chemistry and Physics, La Trobe Institute for Molecular Science, La Trobe University, Melbourne, Victoria, Australia 3086*; orcid.org/0000-0002-0007-4486

Jason L. Dutton − *Department of Chemistry and Physics, La Trobe Institute for Molecular Science, La Trobe University, Melbourne, Victoria, Australia 3086*; orcid.org/0000-0002-0361-4441

Complete contact information is available at: https://pubs.acs.org/10.1021/acs.inorgchem.1c02800

Author Contributions

§G.K.W. and K.R. are co-first authors and contributed equally to this work.

Notes

The authors declare no competing financial interest.

■ ACKNOWLEDGMENTS

The authors are grateful to Baylor University, the Welch Foundation (Grant AA-1846), the National Science Foundation for a CAREER Award (Award 1753025), and the Australian Research Council (FT16010007 and DP20010013) for their generous support of this work. The authors thank John R. Tidwell for assistance with X-ray crystallography. The generous allocation of computing resources by the National Computational Infrastructure (NCI), Intersect, and La Trobe University is acknowledged.

■ REFERENCES

(1) Zeise, W. C. Von der Wirkung zwischen Platinchlorid und Alkohol, und von den dabei entstehenden neuen Substanzen. *Ann. Phys.* **1831**, *97*, 497−541.

(2) Black, M.; Mais, R. H. B.; Owston, P. G. The crystal and molecular structure of Zeise's salt, $KPtCl_3.C_2H_4.H_2O$. *Acta Crystallogr., Sect. B: Struct. Crystallogr. Cryst. Chem.* **1969**, *25*, 1753−1759.

(3) Fischer, E. O.; Pfab, W. Cyclopentadien-Metallkomplexe, ein neuer Typ metallorganischer Verbindungen. *Z. Naturforsch., B: J. Chem. Sci.* **1952**, *7b*, 377−379.

(4) Kealy, T. J.; Pauson, P. L. A New Type of Organo-Iron Compound. *Nature* **1951**, *168*, 1039−1040.

(5) Miller, S. A.; Tebboth, J. A.; Tremaine, J. F. 114. Dicyclopentadienyliron. *J. Chem. Soc.* **1952**, 632−635.

(6) Ruch, E.; Fischer, E. O. Notizen: Zur Frage der Bindung im Dicyclopentadienyl-eisen. *Z. Naturforsch., B: J. Chem. Sci.* **1952**, *7b*, 676−676.

(7) Wilkinson, G.; Rosenblum, M.; Whiting, M. C.; Woodward, R. B. The Structure of Iron Bis-Cyclopentadienyl. *J. Am. Chem. Soc.* **1952**, *74*, 2125−2126.

(8) Baier, M. C.; Zuideveld, M. A.; Mecking, S. Post-Metallocenes in the Industrial Production of Polyolefins. *Angew. Chem., Int. Ed.* **2014**, *53*, 9722−9744.

(9) Green, J. C. Bent metallocenes revisited. *Chem. Soc. Rev.* **1998**, *27*, 263−272.

(10) Green, M. L. H.; Ng, D. K. P. Cycloheptatriene and -enyl Complexes of the Early Transition Metals. *Chem. Rev.* **1995**, *95*, 439−473.

(11) Malenov, D. P.; Zarić, S. D. Stacking interactions of aromatic ligands in transition metal complexes. *Coord. Chem. Rev.* **2020**, *419*, 213338.
(12) Pampaloni, G. Aromatic hydrocarbons as ligands. Recent advances in the synthesis, the reactivity and the applications of bis(η^6-arene) complexes. *Coord. Chem. Rev.* **2010**, *254*, 402−419.
(13) Williams, L. J.; Bhonoah, Y.; Wilkinson, L. A.; Walton, J. W. As Nice as π: Aromatic Reactions Activated by π-Coordination to Transition Metals. *Chem. - Eur. J.* **2021**, *27*, 3650−3660.
(14) Ashe, A. J., III; Shu, P. 1-Phenylborabenzene anion. *J. Am. Chem. Soc.* **1971**, *93*, 1804−1805.
(15) Herberich, G. E.; Greiss, G.; Heil, H. F. A Novel Aromatic Boron Heterocycle as Ligand in a Transition Metal π-Complex. *Angew. Chem., Int. Ed. Engl.* **1970**, *9*, 805−806.
(16) Herberich, G. E.; Ohst, H. Borabenzene Metal Complexes. *Adv. Organomet. Chem.* **1986**, *25*, 199−236.
(17) Ashe, A. J., III; Al-Ahmad, S.; Fang, X. Boratabenzenes: from chemical curiosities to promising catalysts. *J. Organomet. Chem.* **1999**, *581*, 92−97.
(18) Fu, G. C. The chemistry of borabenzenes (1986−2000). *Adv. Organomet. Chem.* **2001**, *47*, 101−119.
(19) Cui, P.; Chen, Y. Boratabenzene rare-earth metal complexes. *Coord. Chem. Rev.* **2016**, *314*, 2−13.
(20) Krummenacher, I.; Schuster, J. K.; Braunschweig, H. Synthesis and Reactivity of Bora- and Borata-Benzenes. *PATAI'S Chemistry of Functional Groups* **2019**, 1−38.
(21) Ashe, A. J., III.; Al-Ahmad, S.; Fang, X.; Kampf, J. W. Bridged Boratabenzene Zirconium Complexes: Analogues of the ansa-Zirconocene Polymerization Catalysts. *Organometallics* **1998**, *17*, 3883−3888.
(22) Komon, Z. J. A.; Bazan, G. C. Ethylene oligomerization and polymerization catalysts supported by boratabenzene ligands. In *Contemporary Boron Chemistry*; The Royal Society of Chemistry, 2000; pp 3−9.
(23) Meng, Y.-S.; Wang, C.-H.; Zhang, Y.-Q.; Leng, X.-B.; Wang, B.-W.; Chen, Y.-F.; Gao, S. (Boratabenzene)(cyclooctatetraenyl) lanthanide complexes: a new type of organometallic single-ion magnet. *Inorg. Chem. Front.* **2016**, *3*, 828−835.
(24) Perez, V.; Audet, P.; Bi, W.; Fontaine, F.-G. Phosphidoboratabenzene−rhodium(i) complexes as precatalysts for the hydrogenation of alkenes at room temperature and atmospheric pressure. *Dalton Trans.* **2016**, *45*, 2130−2137.
(25) Huttner, G.; Krieg, B.; Gartzke, W. Übergangsmetallkomplexe cyclischer π-Liganden, V. Kristall-und Molekülstrukturen von zwei, Borabenzol"□-Derivaten: Bis(1-methoxyborinato)kobalt und Bis(1-methylborinato)kobalt. *Chem. Ber.* **1972**, *105*, 3424−3436.
(26) Huttner, G.; Gartzke, W. Übergangsmetallkomplexe cyclischer π-Liganden, X. Kristall- und Molekülstrukturen von zwei "Borabenzol"□ -Derivaten: Di-μ-carbonyl-dicarbonylbis(1-methylborinato)-dieisen und Tricarbonyl(1-phenylborinato)mangan. *Chem. Ber.* **1974**, *107*, 3786−3799.
(27) Sperry, C. K.; Cotter, W. D.; Lee, R. A.; Lachicotte, R. J.; Bazan, G. C. Tantalum Borollide Trichloride: A Versatile Entry into Tantalum Borollide Complexes. *J. Am. Chem. Soc.* **1998**, *120*, 7791−7805.
(28) Rogers, J. S.; Lachicotte, R. J.; Bazan, G. C. Alkoxy- and Aryloxyboratabenzene Complexes of Zirconium. *J. Am. Chem. Soc.* **1999**, *121* (6), 1288−1298.
(29) Ashe, A. J., III; Al-Ahmad, S.; Fang, X.; Kampf, J. W. Conformational Properties of Boron-Bridged Dimethylethylenediamino Bis(boratabenzene) Zirconium(IV) and Iron(II) Complexes. *Organometallics* **2001**, *20*, 468−473.
(30) Nie, Y.; Pritzkow, H.; Hu, C.; Oeser, T.; Bach, B.; Müller, T.; Siebert, W. Ruthenocene Analogues with a Novel C_5B_2 Ligand: (η^7-4-Borataborepine)(η^5-pentamethylcyclopentadienyl)ruthenium Complexes. *Angew. Chem., Int. Ed.* **2005**, *44*, 632−634.
(31) Ghesner, I.; Piers, W. E.; Parvez, M.; McDonald, R. Synthesis and coordination chemistry of 2,2′-diboratabiphenyls. *Can. J. Chem.* **2006**, *84*, 81−92.
(32) Pammer, F.; Lalancette, R. A.; Jäkle, F. Metallopolymers Featuring Boratabenzene Iron Complexes. *Chem. - Eur. J.* **2011**, *17*, 11280−11289.
(33) Macha, B. B.; Boudreau, J.; Maron, L.; Maris, T.; Fontaine, F.-G. Coordination of a Di-tert-butylphosphidoboratabenzene Ligand to Electronically Unsaturated Group 10 Transition Metals. *Organometallics* **2012**, *31*, 6428−6437.
(34) Mushtaq, A.; Bi, W.; Légaré, M.-A.; Fontaine, F.-G. Synthesis and Reactivity of Novel Mesityl Boratabenzene Ligands and Their Coordination to Transition Metals. *Organometallics* **2014**, *33*, 3173−3181.
(35) Ashe, A. J., III; Kampf, J. W.; Müller, C.; Schneider, M. Aminoboratabenzenes. An Evaluation of the Exocyclic B−N Interaction. *Organometallics* **1996**, *15*, 387−393.
(36) Sperry, C. K.; Rodriguez, G.; Bazan, G. C. Synthesis of two tantalum complexes bearing cyclopentadienyl analogs. *J. Organomet. Chem.* **1997**, *548*, 1−7.
(37) Auvray, N.; Basu Baul, T. S.; Braunstein, P.; Croizat, P.; Englert, U.; Herberich, G. E.; Welter, R. Organometallic building blocks with amino-substituted cyclopentadienyl and boratabenzene ligands for the synthesis of heterometallic complexes and clusters. *Dalton Trans.* **2006**, 2950−2958.
(38) Yuan, Y.; Chen, Y.; Li, G.; Xia, W. Reactions of Boratabenzene Yttrium Complexes with $KN(SiMe_3)_2$: Salt Elimination and π-Ligand Displacement. *Organometallics* **2008**, *27*, 6307−6312.
(39) Bartholome, T. A.; Kaur, A.; Wilson, D. J. D.; Dutton, J. L.; Martin, C. D. The 9-Borataphenanthrene Anion. *Angew. Chem., Int. Ed.* **2020**, *59*, 11470−11476.
(40) Báez-Grez, R.; Pino-Rios, R. Borataalkene or boratabenzene? Understanding the aromaticity of 9-borataphenanthrene anions and its central ring. *New J. Chem.* **2020**, *44*, 18069−18073.
(41) Bartholome, T. A.; Martinez, J. J.; Kaur, A.; Wilson, D. J. D.; Dutton, J. L.; Martin, C. D. Borataalkene Hydrofunctionalization Reactions. *Organometallics* **2021**, *40*, 1966−1973.
(42) Corro, M.; Salvado, O.; González, S.; Dominguez-Molano, P.; Fernández, E. Reactivity Trends with Borylalkyl Copper(I) Species. *Eur. J. Inorg. Chem.* **2021**, *2021*, 2802−2813.
(43) Matteson, D. S.; Moody, R. J. Carbanions from deprotonation of gem-diboronic esters. *J. Am. Chem. Soc.* **1977**, *99*, 3196−3197.
(44) Matteson, D. S.; Arne, K. Carbanions from deprotonation of alpha-(phenylthio)alkaneboronic esters. *J. Am. Chem. Soc.* **1978**, *100*, 1325−1326.
(45) Matteson, D. S.; Moody, R. J. Deprotonation of 1,1-diboronic esters and reactions of the carbanions with alkyl halides and carbonyl compounds. *Organometallics* **1982**, *1*, 20−28.
(46) Pelter, A.; Singaram, B.; Williams, L.; Wilson, J. W. The dimesitylboron group in organic synthesis 1. Introduction. *Tetrahedron Lett.* **1983**, *24*, 623−626.
(47) Knochel, P. A new approach to boron-stabilized organometallics. *J. Am. Chem. Soc.* **1990**, *112*, 7431−7433.
(48) Murray, S. A.; Green, J. C.; Tailor, S. B.; Meek, S. J. Enantio- and Diastereoselective 1,2-Additions to α-Ketoesters with Diborylmethane and Substituted 1,1-Diborylalkanes. *Angew. Chem., Int. Ed.* **2016**, *55*, 9065−9069.
(49) Murray, S. A.; Liang, M. Z.; Meek, S. J. Stereoselective Tandem Bis-Electrophile Couplings of Diborylmethane. *J. Am. Chem. Soc.* **2017**, *139*, 14061−14064.
(50) Maza, R. J.; Carbó, J. J.; Fernández, E. Borata-Alkene Species as Nucleophilic Reservoir. *Adv. Synth. Catal.* **2021**, *363*, 2274−2289.
(51) Waas, J. R.; Sidduri, A.; Knochel, P. Preparation and reactions of 1,1-zinc, boron and 1,1-copper, boron alkenyl bimetallics. *Tetrahedron Lett.* **1992**, *33*, 3717−3720.
(52) Sakai, M.; Saito, S.; Kanai, G.; Suzuki, A.; Miyaura, N. Olefination and hydroxymethylation of aldehydes using Knochel's (dialkoxyboryl)methylcopper reagents. *Tetrahedron* **1996**, *52*, 915−924.
(53) Laitar, D. S.; Tsui, E. Y.; Sadighi, J. P. Copper(I) β-Boroalkyls from Alkene Insertion: Isolation and Rearrangement. *Organometallics* **2006**, *25*, 2405−2408.

https://doi.org/10.1021/acs.inorgchem.1c02800
Inorg. Chem. 2021, 60, 18981−18989

(54) Joannou, M. V.; Moyer, B. S.; Meek, S. J. Enantio- and Diastereoselective Synthesis of 1,2-Hydroxyboronates through Cu-Catalyzed Additions of Alkylboronates to Aldehydes. *J. Am. Chem. Soc.* **2015**, *137*, 6176−6179.
(55) Park, J.; Lee, Y.; Kim, J.; Cho, S. H. Copper-Catalyzed Diastereoselective Addition of Diborylmethane to N-tert-Butanesulfinyl Aldimines: Synthesis of β-Aminoboronates. *Org. Lett.* **2016**, *18*, 1210−1213.
(56) Shi, Y.; Hoveyda, A. H. Catalytic SN2′- and Enantioselective Allylic Substitution with a Diborylmethane Reagent and Application in Synthesis. *Angew. Chem., Int. Ed.* **2016**, *55*, 3455−3458.
(57) Miralles, N.; Gómez, J. E.; Kleij, A. W.; Fernández, E. Copper-Mediated SN2′ Allyl−Alkyl and Allyl−Boryl Couplings of Vinyl Cyclic Carbonates. *Org. Lett.* **2017**, *19*, 6096−6099.
(58) Kim, J.; Ko, K.; Cho, S. H. Diastereo- and Enantioselective Synthesis of β-Aminoboronate Esters by Copper(I)-Catalyzed 1,2-Addition of 1,1-Bis[(pinacolato)boryl]alkanes to Imines. *Angew. Chem., Int. Ed.* **2017**, *56*, 11584−11588.
(59) Jang, W. J.; Yun, J. Catalytic Asymmetric Conjugate Addition of a Borylalkyl Copper Complex for Chiral Organoboronate Synthesis. *Angew. Chem., Int. Ed.* **2019**, *58*, 18131−18135.
(60) Sun, Y.; Zhou, Y.; Shi, Y.; del Pozo, J.; Torker, S.; Hoveyda, A. H. Copper−Hydride-Catalyzed Enantioselective Processes with Allenyl Boronates. Mechanistic Nuances, Scope, and Utility in Target-Oriented Synthesis. *J. Am. Chem. Soc.* **2019**, *141*, 12087−12099.
(61) Joannou, M. V.; Moyer, B. S.; Goldfogel, M. J.; Meek, S. J. Silver(I)-Catalyzed Diastereoselective Synthesis of anti-1,2-Hydroxyboronates. *Angew. Chem., Int. Ed.* **2015**, *54*, 14141−14145.
(62) Arrowsmith, M.; Auerhammer, D.; Bertermann, R.; Braunschweig, H.; Celik, M. A.; Erdmannsdörfer, J.; Krummenacher, I.; Kupfer, T. From Borane to Borylene without Reduction: Ambiphilic Behavior of a Monovalent Silylisonitrile Boron Species. *Angew. Chem., Int. Ed.* **2017**, *56*, 11263−11267.
(63) Phillips, N. A.; Coates, G. J.; White, A. J. P.; Crimmin, M. R. Defluoroalkylation of sp3 C−F Bonds of Industrially Relevant Hydrofluoroolefins. *Chem. - Eur. J.* **2020**, *26*, 5365−5368.
(64) Phillips, N. A.; Kong, R. Y.; White, A. J. P.; Crimmin, M. R. Group 11 Borataalkene Complexes: Models for Alkene Activation. *Angew. Chem., Int. Ed.* **2021**, *60*, 12013−12019.
(65) Herberich, G. E.; Becker, H. J.; Carsten, K.; Engelke, C.; Koch, W. Derivate des Borabenzols, VIII: Ein neuer Weg zu Alkalimetallborinaten. Synthesen von Ruthenium-, Osmium-, Rhodium- und Platin-Verbindungen mit Borinat-Liganden. *Chem. Ber.* **1976**, *109*, 2382−2388.
(66) Herberich, G. E.; Hessner, B. Eine neue synthese von 1,4-Dibora-2,5-cyclohexadienen. *J. Organomet. Chem.* **1978**, *161*, C36−C40.
(67) Herberich, G. E.; Schmidt, B.; Englert, U.; Wagner, T. Borabenzene derivatives. 21. 2,4-Pentadienylboranes as key intermediates of a novel route to boracyclohexadienes and boratabenzenes. Structure of [Li(TMPDA)]($C_5H_5BNMe_2$). *Organometallics* **1993**, *12*, 2891−2893.
(68) Herberich, G. E.; Schmidt, B.; Englert, U. Borabenzene Derivatives. 22. Synthesis of Boratabenzene Salts from 2,4-Pentadienylboranes. Structure of [NMe_3Ph][C_5H_5BMe]. *Organometallics* **1995**, *14*, 471−480.
(69) Herberich, G. E.; Englert, U.; Schmidt, M. U.; Standt, R. Borabenzene Derivatives. 23.1 New Synthetic Entry into Borabenzene Chemistry via Doubly Kaliated Pentadienes: Synthesis of 1-(Dimethylamino)-3-methylene-1,2,3,6-tetrahydroborinines and Lithium 1-(Dimethylamino)boratabenzene Derivatives. *Organometallics* **1996**, *15*, 2707−2712.
(70) Hoic, D. A.; Wolf, J. R.; Davis, W. M.; Fu, G. C. Chemistry of Borabenzene: Efficient and General Synthesis of New Neutral Borabenzene−Ligand Complexes. *Organometallics* **1996**, *15*, 1315−1318.
(71) Herberich, G. E.; Cura, E.; Ni, J. A new synthetic route to 2-boratanaphthalenes. *Inorg. Chem. Commun.* **1999**, *2*, 503−506.
(72) Herberich, G. E.; Englert, U.; Ganter, B.; Pons, M.; Wang, R. Borabenzene Derivatives. 28. Pinene-Fused Dihydroborinines, Boratabenzenes, and a Borabenzene−Pyridine Adduct1. *Organometallics* **1999**, *18*, 3406−3413.
(73) Ashe, A. J., III; Fang, X.; Kampf, J. W. Synthesis and Properties of 1-Substituted 1-Boratanaphthalenes. *Organometallics* **1999**, *18*, 466−473.
(74) Légaré, M.-A.; Bélanger-Chabot, G.; De Robillard, G.; Languérand, A.; Maron, L.; Fontaine, F.-G. Insights into the Formation of Borabenzene Adducts via Ligand Exchange Reactions and TMSCl Elimination from Boracyclohexadiene Precursors. *Organometallics* **2014**, *33*, 3596−3606.
(75) Braunschweig, H.; Hupp, F.; Krummenacher, I.; Mailänder, L.; Rauch, F. Ring Expansions of Boroles with Diazo Compounds: Steric Control of C or N Insertion and Aromatic/Nonaromatic Products. *Chem. - Eur. J.* **2015**, *21*, 17844−17849.
(76) Bartholome, T. A.; Bluer, K. R.; Martin, C. D. Successive carbene insertion into 9-phenyl-9-borafluorene. *Dalton Trans.* **2019**, *48*, 6319−6322.
(77) Fagan, P. J.; Burns, E. G.; Calabrese, J. C. Synthesis of boroles and their use in low-temperature Diels-Alder reactions with unactivated alkenes. *J. Am. Chem. Soc.* **1988**, *110*, 2979−2981.
(78) Fagan, P. J.; Nugent, W. A.; Calabrese, J. C. Metallacycle Transfer from Zirconium to Main Group Elements: A Versatile Synthesis of Heterocycles. *J. Am. Chem. Soc.* **1994**, *116*, 1880−1889.
(79) Baker, J. J.; Al Furaiji, K. H. M.; Liyanage, O. T.; Wilson, D. J. D.; Dutton, J. L.; Martin, C. D. Diverse Reactivity of Dienes with Pentaphenylborole and 1-Phenyl-2,3,4,5-Tetramethylborole Dimer. *Chem. - Eur. J.* **2019**, *25*, 1581−1587.
(80) Su, X.; Baker, J. J.; Martin, C. D. Dimeric boroles: effective sources of monomeric boroles for heterocycle synthesis. *Chem. Sci.* **2020**, *11*, 126−131.
(81) Wright, A. M.; Irving, B. J.; Wu, G.; Meijer, A. J. H. M.; Hayton, T. W. A Copper(I)−Arene Complex With an Unsupported η^6 Interaction. *Angew. Chem., Int. Ed.* **2015**, *54*, 3088−3091.
(82) Huang, J.; Schanz, H.-J.; Stevens, E. D.; Nolan, S. P. Stereoelectronic Effects Characterizing Nucleophilic Carbene Ligands Bound to the Cp*RuCl (Cp* = η^5-C_5Me_5) Moiety: A Structural and Thermochemical Investigation. *Organometallics* **1999**, *18*, 2370−2375.
(83) Trnka, T. M.; Grubbs, R. H. The Development of L_2X_2RuCHR Olefin Metathesis Catalysts: An Organometallic Success Story. *Acc. Chem. Res.* **2001**, *34*, 18−29.
(84) Herrmann, W. A. N-Heterocyclic Carbenes: A New Concept in Organometallic Catalysis. *Angew. Chem., Int. Ed.* **2002**, *41*, 1290−1309.
(85) Samojłowicz, C.; Bieniek, M.; Grela, K. Ruthenium-Based Olefin Metathesis Catalysts Bearing N-Heterocyclic Carbene Ligands. *Chem. Rev.* **2009**, *109*, 3708−3742.
(86) Liu, M.; Yang, I.; Buckley, B.; Lee, J. K. Proton Affinities of Phosphines versus N-Heterocyclic Carbenes. *Org. Lett.* **2010**, *12*, 4764−4767.
(87) Zhao, Y.; Truhlar, D. G. The M06 suite of density functionals for main group thermochemistry, thermochemical kinetics, noncovalent interactions, excited states, and transition elements: two new functionals and systematic testing of four M06-class functionals and 12 other functionals. *Theor. Chem. Acc.* **2008**, *120*, 215−241.
(88) Weigend, F.; Ahlrichs, R. Balanced basis sets of split valence, triple zeta valence and quadruple zeta valence quality for H to Rn: Design and assessment of accuracy. *Phys. Chem. Chem. Phys.* **2005**, *7*, 3297−3305.
(89) Barone, V.; Cossi, M. Quantum Calculation of Molecular Energies and Energy Gradients in Solution by a Conductor Solvent Model. *J. Phys. Chem. A* **1998**, *102*, 1995−2001.
(90) Neese, F. Software update: the ORCA program system, version 4.0. *Wiley Interdiscip. Rev.: Comput. Mol. Sci.* **2018**, *8*, e1327.
(91) te Velde, G.; Bickelhaupt, F. M.; Baerends, E. J.; Fonseca Guerra, C.; van Gisbergen, S. J. A.; Snijders, J. G.; Ziegler, T. Chemistry with ADF. *J. Comput. Chem.* **2001**, *22*, 931−967.

https://doi.org/10.1021/acs.inorgchem.1c02800
Inorg. Chem. 2021, 60, 18981−18989

(92) Baerends, E. J.; Ziegler, T.; Atkins, A. J.; Autschbach, J.; Baseggio, O.; Bashford, D.; Bérces, A.; Bickelhaupt, F. M.; Bo, C.; Boerrigter, P. M.; Cavallo, L.; Daul, C.; Chong, D. P.; Chulhai, D. V.; Deng, L.; Dickson, R. M.; Dieterich, J. M.; Ellis, D. E.; Faassen, M. v.; Fan, L.; Fischer, T. H.; Förster, A.; Guerra, C. F.; Franchini, M.; Ghysels, A.; Giammona, A.; Gisbergen, S. J. A. v.; Goez, A.; Götz, A. W.; Groeneveld, J. A.; Gritsenko, O. V.; Grüning, M.; Gusarov, S.; Harris, F. E.; Hoek, P. v. d.; Hu, Z.; Jacob, C. R.; Jacobsen, H.; Jensen, L.; Joubert, L.; Kaminski, J. W.; Kessel, G. v.; König, C.; Kootstra, F.; Kovalenko, A.; Krykunov, M. V.; Lenthe, E. v.; McCormack, D. A.; Michalak, A.; Mitoraj, M.; Morton, S. M.; Neugebauer, J.; Nicu, V. P.; Noodleman, L.; Osinga, V. P.; Patchkovskii, S.; Pavanello, M.; Peeples, C. A.; Philipsen, P. H. T.; Post, D.; Pye, C. C.; Ramanantoanina, H.; Ramos, P.; Ravenek, W.; Rodríguez, J. I.; Ros, P.; Rüger, R.; Schipper, P. R. T.; Schlüns, D.; Schoot, H. v.; Schreckenbach, G.; Seldenthuis, J. S.; Seth, M.; Snijders, J. G.; Solà, M.; Stener, M.; Swart, M.; Swerhone, D.; Tognetti, V.; Velde, G. t.; Vernooijs, P.; Versluis, L.; Visscher, L.; Visser, O.; Wang, F.; Wesolowski, T. A.; Wezenbeek, E. M. v.; Wiesenekker, G.; Wolff, S. K.; Woo, T. K.; Yakovlev, A. L. *ADF 2020, SCM, Theoretical Chemistry*; Vrije Universiteit: Amsterdam, http://www.scm.com, 2020.

(93) Johnson, E. R.; Keinan, S.; Mori-Sánchez, P.; Contreras-García, J.; Cohen, A. J.; Yang, W. Revealing Noncovalent Interactions. *J. Am. Chem. Soc.* **2010**, *132*, 6498−6506.

(94) Frisch, M. J.; Trucks, G. W.; Schlegel, H. B.; Scuseria, G. E.; Robb, M. A.; Cheeseman, J. R.; Scalmani, G.; Barone, V.; Petersson, G. A.; Nakatsuji, H.; Li, X.; Caricato, M.; Marenich, A. V.; Bloino, J.; Janesko, B. G.; Gomperts, R.; Mennucci, B.; Hratchian, H. P.; Ortiz, J. V.; Izmaylov, A. F.; Sonnenberg, J. L.; Williams; Ding, F.; Lipparini, F.; Egidi, F.; Goings, J.; Peng, B.; Petrone, A.; Henderson, T.; Ranasinghe, D.; Zakrzewski, V. G.; Gao, J.; Rega, N.; Zheng, G.; Liang, W.; Hada, M.; Ehara, M.; Toyota, K.; Fukuda, R.; Hasegawa, J.; Ishida, M.; Nakajima, T.; Honda, Y.; Kitao, O.; Nakai, H.; Vreven, T.; Throssell, K.; Montgomery, J. A., Jr.; Peralta, J. E.; Ogliaro, F.; Bearpark, M. J.; Heyd, J. J.; Brothers, E. N.; Kudin, K. N.; Staroverov, V. N.; Keith, T. A.; Kobayashi, R.; Normand, J.; Raghavachari, K.; Rendell, A. P.; Burant, J. C.; Iyengar, S. S.; Tomasi, J.; Cossi, M.; Millam, J. M.; Klene, M.; Adamo, C.; Cammi, R.; Ochterski, J. W.; Martin, R. L.; Morokuma, K.; Farkas, O.; Foresman, J. B.; Fox, D. J. *Gaussian 16*; Gaussian, Inc.: Wallingford, CT, 2016.

(95) Stanger, A. Nucleus-Independent Chemical Shifts (NICS): Distance Dependence and Revised Criteria for Aromaticity and Antiaromaticity. *J. Org. Chem.* **2006**, *71*, 883−893.

(96) Ligand competition experiments were conducted via 1:1 reactions of the coinage metal complexes (**1**·$MPPh_3$ or **2**·$MPPh_3$) with the other ligand (**1**·K or **2**·K) in THF/benzene at room temperature (see page S89 of the Supporting Information). For both copper reactions, the peaks corresponding to free **1**·K and complexed **2**·$CuPPh_3$ were observed in the ^{11}B NMR spectra, confirming **2**·$CuPPh_3$ is favored over **1**·$CuPPh_3$. The reactions with the silver complexes led to complex mixtures, indicating that clean ligand exchange did not occur. The reactions with the gold complexes resulted in a mixture of **1**·$AuPPh_3$ and **2**·$AuPPh_3$ as observed in the $^{31}P\{^1H\}$ NMR spectrum that indicates an equilibrium between **1**·$AuPPh_3$ and **2**·$AuPPh_3$.

https://doi.org/10.1021/acs.inorgchem.1c02800
Inorg. Chem. 2021, 60, 18981−18989